Korean J. Chem. Eng., 26(4), 1137-1143 (2009)
DOI: 10.1007/s11814-009-0189-4

Numerical simulation of the influence of over fire air position on the combustion in a single furnace boiler with dual circle firing

Hiu Liu*,,†, Nana Xin**, Qingxi Cao**, Long Sha**, Dezhi Sun*, and Shaohua Wu****

*Postdoctoral Station of Environmental Science and Engineering, Harbin Institute of Technology, Harbin 150090, P. R. China
**School of Energy Science and Engineering, Harbin Institute of Technology, Harbin 150001, P. R. China
(*Received 28 July 2008 • accepted 5 January 2009*)

Abstract−The Computational fluid dynamics (CFD) code PHOENICS is applied to simulate and evaluate the combustion process within the furnace of a 1,000 MW dual circle tangential firing single furnace lignite-fired ultra supercritical (USC) boiler. The dependence on overfire air (OFA) positioning on the combustion process is studied. The results show that the highest temperature appears on the upside of the burner zone close to the front wall, and the high temperature zone rises with elevated OFA positions. However, the temperature field distributions are similar despite differing OFA positions. The char content near the rear wall is higher than that near the front wall, and below the furnace arch, coal particles concentrate towards the front wall. Also with elevated OFA positions, nitrogen oxide (NO_x) concentrations at the outlet fall, but char content increases. In regard to NO_x emission and char burnout, the suggested optimal distance from the OFA center to the center of the uppermost primary air nozzle should be 6 meters.

Key words: OFA, Combustion, NO_x, Numerical Simulation, Dual Circle Tangential Firing

INTRODUCTION

Recently, in the field of clean coal power generation, USC technology has become a necessary choice for China. For most boiler units taking advantage of the USC technology, the large-scale Π type layout with dual circle tangential firing single furnace system has often been adopted. China's abundant reserve of lignite encourages the development of lignite-fired USC boilers of large capacity. This is exemplified by the current planning of a 1,000 MW dual circle tangential firing single furnace lignite-fired USC boiler.

Staged-air combustion has been widely adopted in existing USC boilers, and is proving to be in general an effective low-NO_x emission process [1], a fact that holds for both air horizontally-staged combustion and air axially-staged combustion. However, when it comes to considering the OFA technique, a key parameter is the actual positioning of the OFA. For all boilers, an optimal OFA position exists which varies depending on differing capacities or differing coal types used in burning. By controlling and adjusting this position while in operation, NO_x emissions can be greatly reduced while simultaneously having less influence on combustion efficiency. Moreover, slagging and high-temperature corrosion can be bought under control [2,3].

Commercial software is universally used in the numerical simulation of furnace combustion processes [4-6]. In reference [6], a 1,000 MW bituminous-fired USC boiler with a single furnace and dual circle tangential firing system from the Yuhuan Plant has been studied by numerical simulation and reasonable results have been obtained. In this paper, the CFD code PHOENICS has been applied in evaluating the combustion process within the furnace of a lignite-fired USC boiler with OFA, and characteristics of temperature distributions, NO_x emissions and char burnout have been obtained. The results of the numerical simulation are used as a reference in improving boiler design.

MODELS AND METHOD

1. Physical Aspects of the Model

The aim is to simulate a 1,000 MW lignite-fired USC boiler with a single furnace and dual circle tangential firing system [7], adopting Π type layout. This boiler has ten levels of primary air nozzles of bias combustion upon which 10 MPS280 type mills are applied, and of which nine are in service when operating at the boiler's maximum continuous rating. The furnace can be vertically divided into two parts, the main combustion zone and the burnout zone. Fig. 1 and Fig. 2 show, respectively, the horizontal arrangement for the burners and the single-line configuration of the burner nozzles.

The computational region spans the cold ash hopper and the inlet of the horizontal flue, contained in a rectangular volume with sides of lengths 17.806 m, 36.623 m and 76.444 m in breadth (X direction), width (Y direction), and height (Z direction), respectively. The specific configuration is shown in Fig. 3. After optimization, the mesh sizes for the numerical calculation are 35 m, 58 m and 115 m in the X, Y, and Z directions, respectively.

The simulations are assumed to be operating at the boiler's maximum continuous rating. As indicated in Fig. 2, the primary air nozzles in levels A1, B1, C1, D1, E1, A2, B2, C2 and D2 were taken as being operational. The coal characteristics employed in each simulation were as shown in Table 1.

2. Mathematical Models

Considering the reliability of the models and the ease of project application, a standard k-ε two-equation model [8,9] was used for

†To whom correspondence should be addressed.
E-mail: liuhui@hit.edu.cn
‡This work was presented at the 7th China -Korea Workshop on Clean Energy Technology held at Taiyuan, Shanxi, China, June 26-28, 2008.

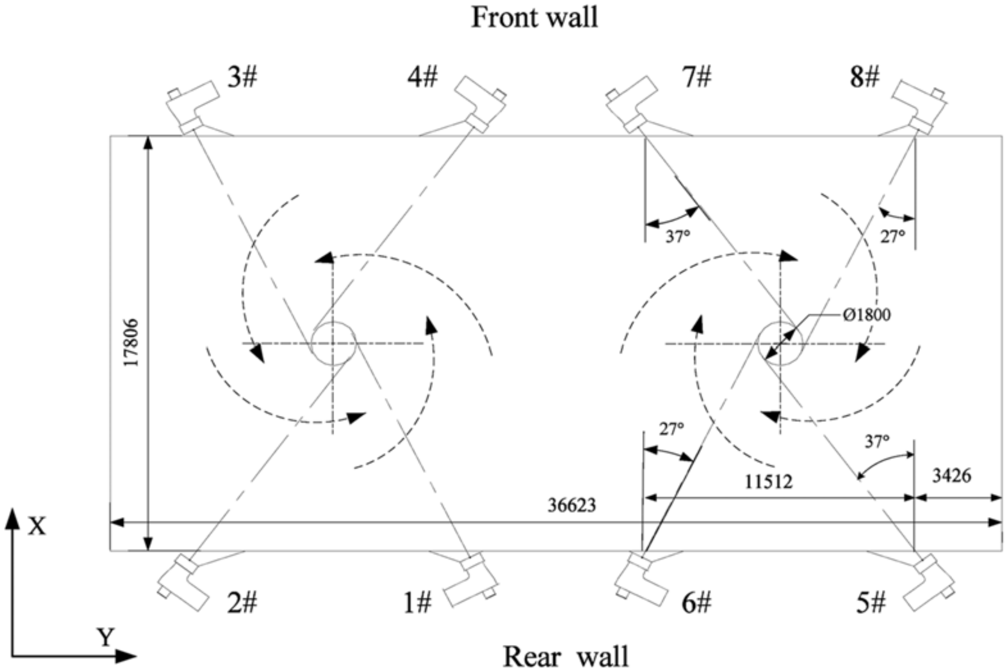

Fig. 1. Horizontal arrangement of the burners.

the simulation of the gas phase turbulence flow, in conjunction with a two fluid model based on the inter-phase slip algorithm (IPSA) simulating the gas-solid two-phase flow, and the six-flux model for radiation. A pulverized coal combustion integration model was employed, wherein the diffusion model was used for moisture evaporation, a single-step reaction model for devolatilization, an EBU-Arrhenius model for the burning of volatile and finally a diffusion/kinetics model for the char combustion. In modelling NO_x emissions, only NO was considered and a post-processing procedure was applied to the NO simulation based on the results of the main combustion process in the furnace. Thermal NO was predicted by using the extended Zeldovich mechanism. The calculation of fuel NO was performed using equations for HCN and NO transport with the reaction mechanisms proposed by De Soete [10]. The influence of char reduction on NO was considered although prompt NO was neglected. The models above, all of which have been validated by experimentation results [11], can quantitatively reflect the combustion process within a furnace of a large pulverized coal boiler and determine gas temperatures and species distributions in the furnace with reasonable precision.

3. Boundary Conditions and Solution Method

The wall boundary constraint was fixed as being non-slip, and the wall temperature set at 460 °C in accord with the temperature of the working fluid inside the water wall and the heat resistance of the tubes. The surface temperature of the platen superheaters near the outlet was set at 640 °C and the emissivity of the water wall surface was chosen with a value of 0.8. The outlet pressure was set to standard atmospheric pressure. The parameters of the burners were also set according to the design parameters for the boiler. Finite difference methods were employed to resolve the differential equations. SIMPLEST [12] arithmetic was used to solve the governing equations in the heterogeneous staggered structured grid system expressed in orthogonal coordinates. After 7000 iterations, convergence was achieved.

RESULTS AND DISCUSSION

1. Case and Parameter Setting

Altogether five scenarios, denoted A1, A2, A3, A4 and A5, are investigated, in which the distance (H) from the uppermost primary air center to the OFA center is set to 3 m, 5 m, 6 m, 7 m and 9 m, respectively. All scenarios are initialized with constant values of total air flux and OFA flux, using a uniform air distribution. The burner inlet parameters in each case are listed in Table 2.

2. Distributions of Temperature Field

The distributions of gas temperature in the central longitudinal section paralleling the two sidewalls of the furnace are shown in Fig. 4 for the five different scenarios. They show that the region between 20 m to 45 m in height constitutes the high temperature zone, the highest temperature appearing at a position approximately 37 m away from the bottom of the furnace and located on the upside of the burner zone in the main combustion zone. The reason for this is seen in the fact that the excess air coefficient in the main combustion zone is less than unity in this region, and the incomplete combustion products continue to react with air from the highest secondary air nozzles, leading to an increase in gas temperatures. In the burnout zone, gas temperatures decrease due to the OFA injection at a lower temperature and an endothermic effect within the heating surface. With elevated OFA position, the high temperature zone shifts upwards.

The figures show that the high temperature zone is close to the front wall, and this is due to the fact that in the dual circle tangential firing furnace the orientation of the two swirling eddies is reverse. The direction of injections from NO.4 and NO.7 nozzles diverge away toward their own swirling centers, thus leaving a large space which is unprotected from low temperature air. Under the impact

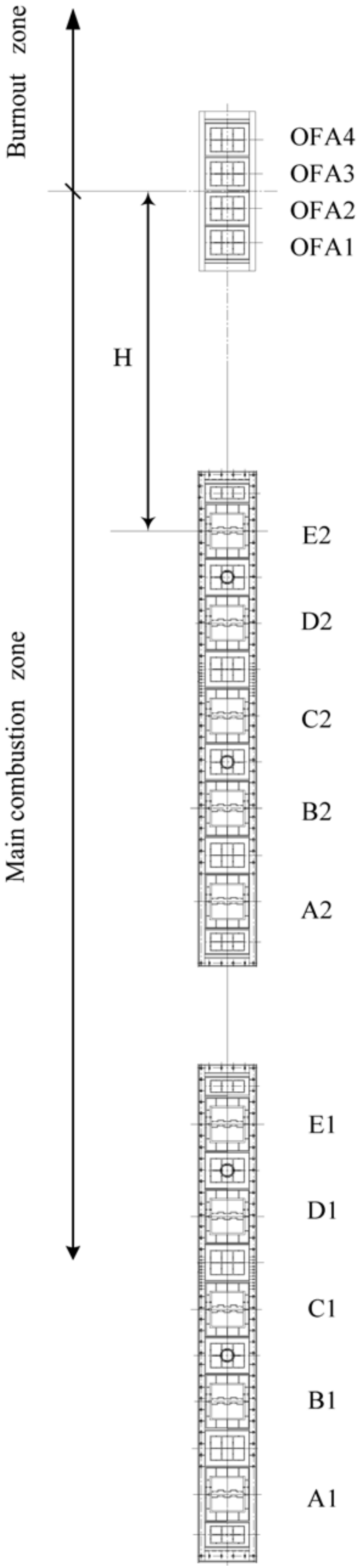

Fig. 2. Configuration of single line burner nozzles.

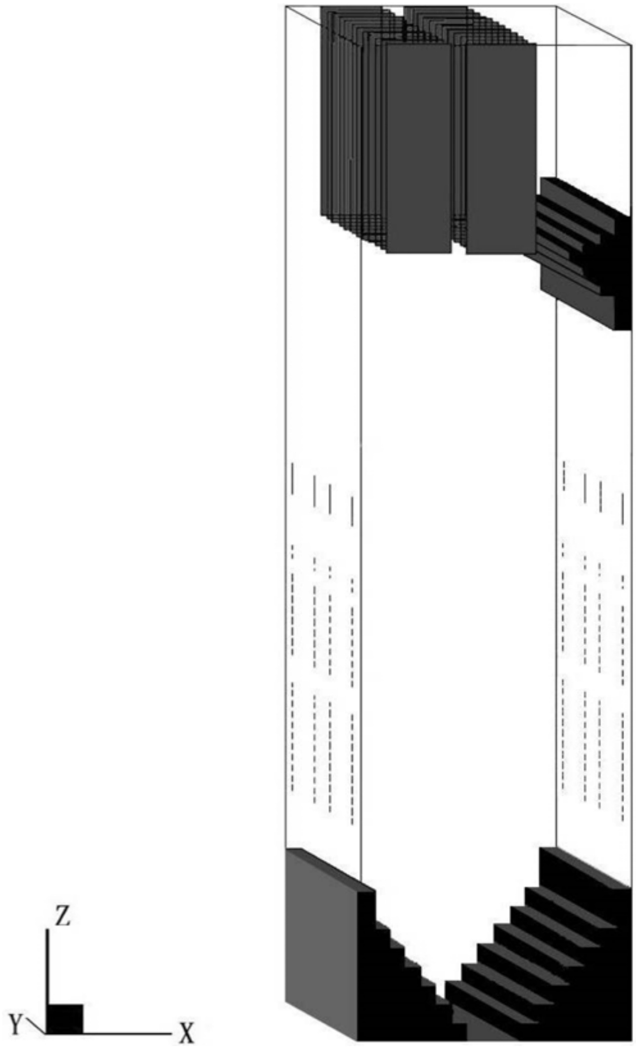

Fig. 3. Computational region of the furnace.

Table 1. Proximate analysis and ultimate analysis of the designed coal

Proximate analysis	Moisture (% as received)	30
	Ash (% as received)	17.97
	Volatile matter (% as received)	23.78
	Fixed carbon (% as received)	28.25
Ultimate analysis	Carbon (% as received)	36.5
	Hydrogen (% as received)	2.6
	Oxygen (% as received)	11.3
	Nitrogen (% as received)	0.63
	Sulfur (% as received)	1
Net heating value (kJ kg^{-1} as received)		13,172

from NO.2 and NO.5 injections, the injections from NO.1 and NO.6 nozzles flow into the space between NO.4 and NO.7 burners. Having been ignited by the upriver flame, gas flows from NO.1 and NO.6 burners develop into a high temperature flame on reaching the space between NO.4 and NO.7 burners, which then leads to higher temperature levels. This is in agreement with observations reported in reference [13].

Fig. 5 shows average gas temperatures in horizontal cross sec-

Table 2. Burner inlet parameters using the designed coal

Primary air velocity (m/s)	26
Secondary air velocity (m/s)	49
OFA velocity (m/s)	60
Pulverized coal mass flux of fuel-rich nozzle (kg/s)	1.36
Pulverized coal mass flux of fuel-lean nozzle (kg/s)	0.9
Primary air temperature (ºC)	65
Secondary air and OFA temperature (ºC)	376.3
Primary air ratio (%)	35
OFA ratio (%)	20.48
Excess air coefficient	1.2

tions along the furnace axis in the five scenarios. Comparisons show that the high temperature zone rises with elevated OFA position. In the burner zone of the main combustion zone and the top region of the burnout zone, the temperature distributions resulting from the different scenarios are similar. Moreover, the injection of OFA will reduce gas temperatures. Fig. 6 shows the average gas temperatures of the furnace outlet in each scenario, indicating that the average temperature of the outlet increases slightly with elevated OFA nozzles. This is in agreement with observations reported in reference [14].

3. Influence on Slagging

The main focus of this paper is the simulation of a lignite-fired boiler using lignite with low ash fusion point, a fuel which is prone to slag. To simulate the prevention of slagging, we selected in the furnace design a lower furnace cross-section thermal load and a lower furnace volume heat load, together with a lower OFA rate, and within the main combustion zone an excess air factor of 0.995, which is close to unity, to avoid slagging triggered by a reducing atmosphere in the main combustion zone. The high temperature zone above

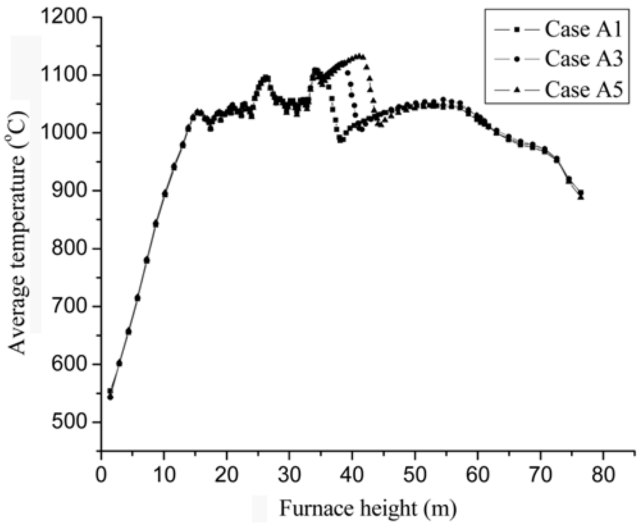

Fig. 5. Cross-sectional gas temperatures averages (ºC) along the furnace height in three scenarios.

the burners would rise with an elevated OFA position, while temperatures would not change significantly. Meanwhile, because the excess air factor of the main combustion zone was close to unity, the reducing atmosphere zone would not increase nor would there be an obvious effect on cross-sectional velocity distributions within the burner zone when OFA position are elevated, as can be seen from Fig. 7. With regard to temperature, reducing atmosphere and aerodynamic field in the boiler, there would be no clear effect of OFA positioning on slagging. Reviewing the results of the calculation, the location most susceptible to slagging was the region near the front wall below the OFA, where temperatures are highest. Because this region of the water wall moves upward as the OFA posi-

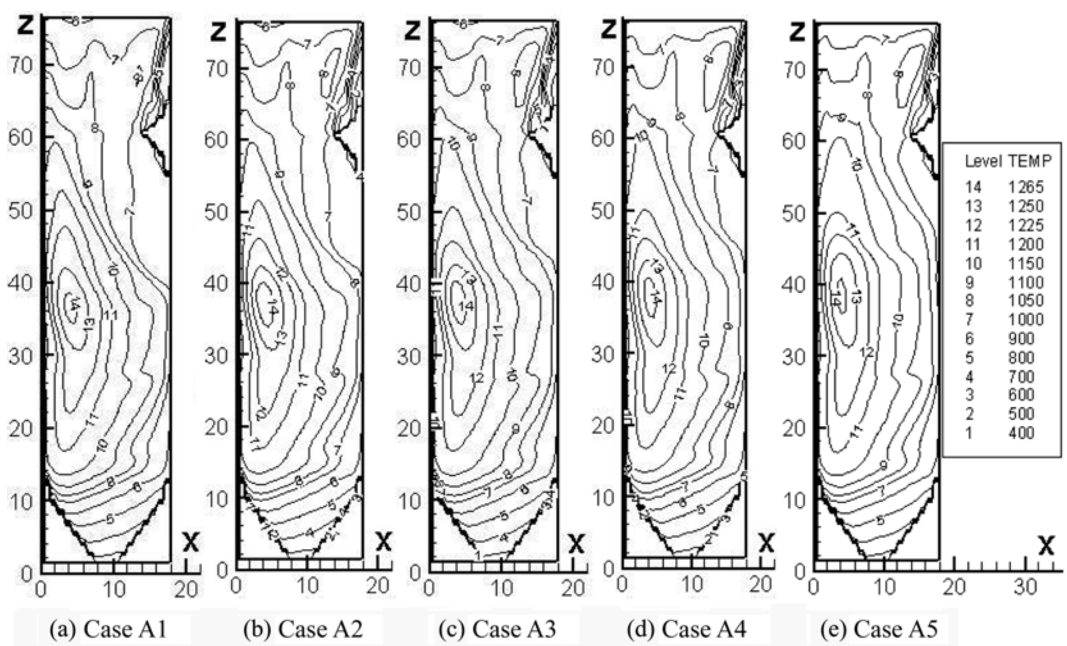

Fig. 4. Gas temperature distributions (ºC) in the central longitudinal section paralleling the two sidewalls of the furnace fin five scenarios corresponding to different OFA positions.

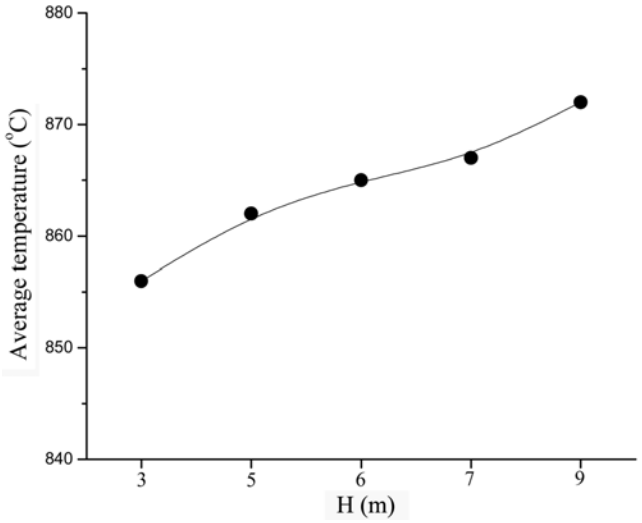

Fig. 6. Average flue gas temperatures (°C) at the outlet in five scenarios.

tion is elevated, consideration should be given to the location of the soot blower in the design phase.

4. Burning Characteristics of Char

Fig. 8 shows the distribution of the char mass fraction in the central longitudinal section, paralleling the two sidewalls of the furnace in the five scenarios. The changes in char content within the burner zone are seen to be similar with varying OFA positions. The char concentration is largest in two areas within the combustion zone because of the firings of the two groups of burner nozzles located there. Moreover, the char content near the rear wall is higher than that near the front wall. Having passed through the OFA nozzles, the char concentration begins to fall gradually with increasing furnace height, which agrees with the analysis of temperature fields. In addition, it also implies that as a result of the influence of the furnace arch above the airflow, in the zone above a height of 45 m along the furnace's central axis, the coal particles concentrate toward the front wall by centrifugal force combustion, and subsequently the average char content at the outlet is very low. Comparing the five scenarios, it can be deduced that for the same cross sections in the region above the OFA nozzles, the char content is a little higher given a higher elevated OFA position. The average char mass fractions at the furnace outlet in different cases are shown in Fig. 9, indicating that in elevating the OFA position, the char content at the outlet increases. The reason for the above results is that an elevated OFA position postpones the mixing of pulverized coal and OFA, which is disadvantageous in char burnout.

5. Emission Characteristics of NO_x

Throughout the simulation, the furnace temperature is set lower than 1,450 °C; therefore, the thermal NO formation is slight and the formation of fuel NO determines the final NO emission of the furnace. Fig. 9 also shows the average NO concentration (mg/m^3, at 6% O_2) at the outlet in different cases, from which we can see that the NO emission decreases with elevated OFA.

An elevated OFA position lengthens the main combustion zone along the furnace's height, which prolongs combustion times for coal particles and deoxidization times for intermediate nitrogenous products, such as HCN, NH_3, etc. [15], thus contributing to the decrease in fuel NO in the main combustion zone. Longer residence times in the fuel-rich zone scarcely contribute in decreasing the NO_x emission concentrations [16]. Therefore, the existence of an optimal OFA position is understandable in light of both NO_x reduction and char burnout.

CONCLUSIONS

There are significant conclusions to be drawn from the numeri-

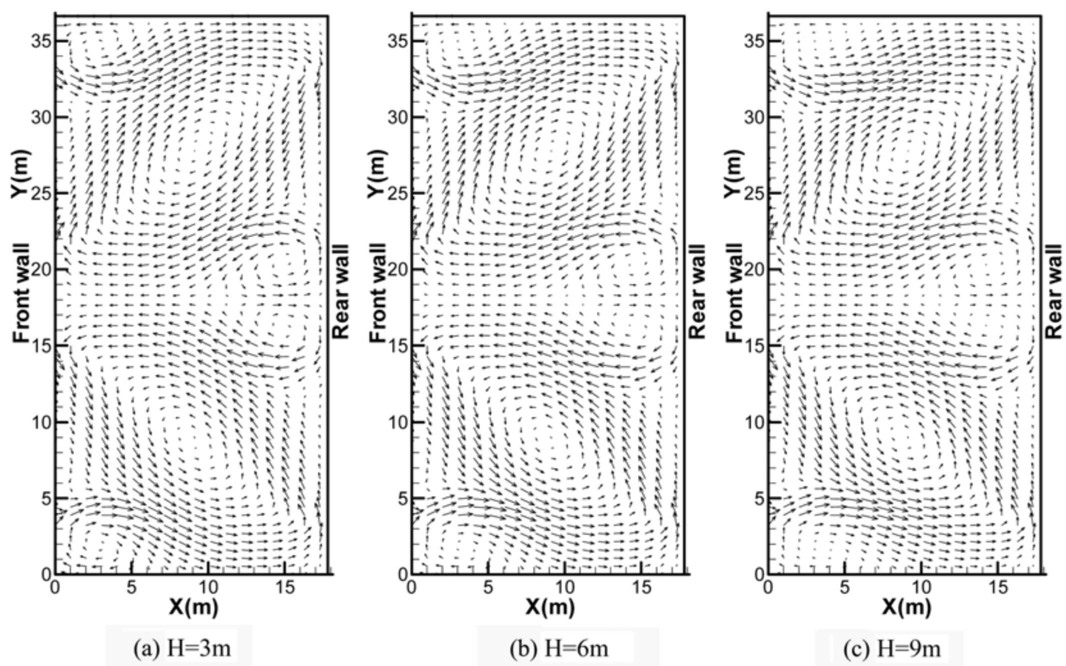

Fig. 7. Cross-sectional velocity distributions in the main burner zone with different OFA positions.

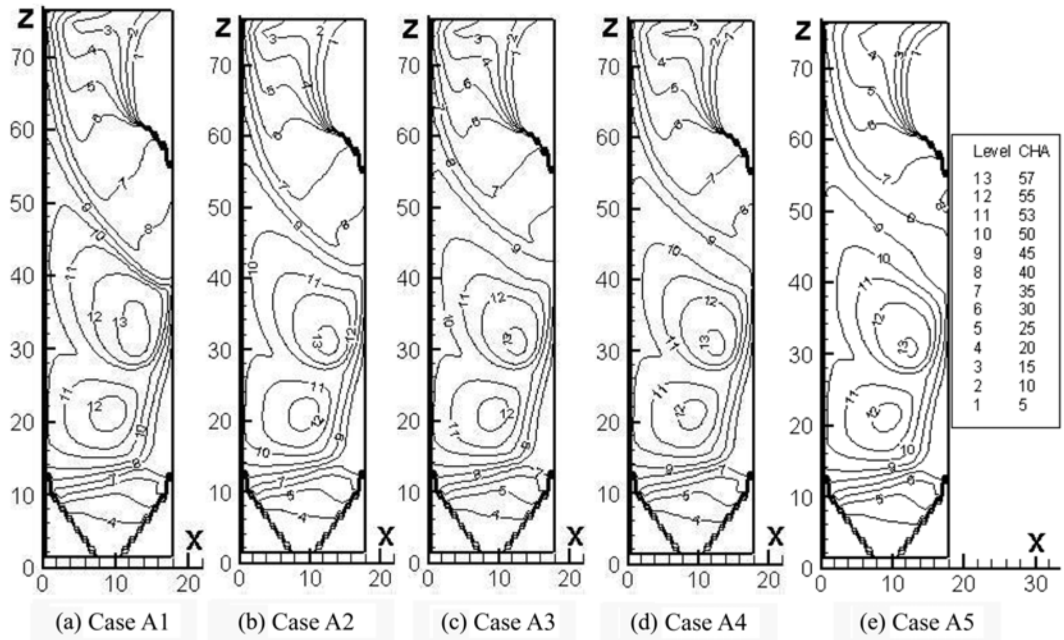

Fig. 8. Distributions of the char mass fraction (%) in the central longitudinal section paralleling the two sidewalls of the furnace in five scenarios.

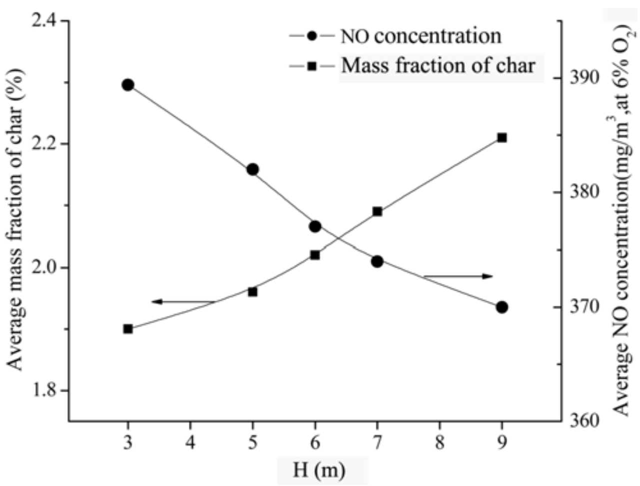

Fig. 9. Average mass fractions of char (%) and average NO concentrations (mg/m^3, at 6% O_2) at the outlet in five scenarios.

cal simulations of the influence of OFA on the combustion in a dual circle tangential firing single furnace boiler:

1. The region between furnace heights of 20 m and 45 m constitutes the high gas temperature zone. The highest temperature appears in the upside of the burner zone, close to the front wall. Moreover, the injection of OFA can reduce furnace temperatures. Elevated OFA position raises the high temperature zone, which in turn leads to a slight increase in the average temperature of the outlet.

2. The char mass fraction is largest in two zones in the combustion zone, and the char content near the rear wall is higher than that near the front wall. Below the furnace arch, coal particles concentrate toward the front wall, and then with the later combustion, char content averages at the outlet are very low. Furthermore, with elevated OFA positions, char content at the outlet increases.

3. NO emissions are lowered with elevated OFA positions. Thus, when considering NO_x emissions and char burnout, the suggested optimal distance from the OFA center to the center of the uppermost primary air nozzle is 6 meters.

ACKNOWLEDGMENTS

This work was supported by the Hi-Tech Research and Development Program of China (863 program) (Contract No.: 2006AA05Z320) and Project HIT.NSRIF.2008.64 supported by Natural Scientific Research Innovation Foundation in Harbin Institute of Technology.

NOMENCLATURE

H : height from upmost primary air nozzle center to center of total OFA nozzles
X : distance from back to front wall of furnace
Y : distance from left to right side wall of furnace
Z : distance from top to bottom of furnace

REFERENCES

1. P. H. Qiu, S. H. Wu, S. Z. Sun, H. Liu, L. B. Yang and G. Z. Wang, *Korean J. Chem. Eng.*, **24**, 683 (2007).
2. S. Li, T. M. Xu, P. Sun, Q. L. Zhou, H. Z. Tan and S. E. Hui, *Fuel*, **87**, 723 (2008).
3. L. K. Huang, Z. Q. Li, R. Sun and J. Zhou, *Fuel Processing Technology*, **87**, 363 (2006).
4. F. Marias, J. R. Puiggali, M. Quintard and R. Pit, *Korean J. Chem. Eng.*, **19**, 28 (2002).
5. H. Y. Park and Y. J. Kim, *Korean J. Chem. Eng.*, **14**, 83 (2007).
6. C. M. Shen, R. Sun and S. H. Wu, *Proceeding of the CSEE*, **26**, 51 (2006) (in Chinese).

7. M. C. Zhang, T. K. Niu and W. D. Fan, *Boiler Technology*, **32**, 1 (2001) (in Chinese).
8. J. R. Fan, X. H. Liang, Q. S. Xu, X. Y. Zhang and K. F. Cen, *Energy*, **22**, 847 (1997).
9. F. C. Lockwood and C. Papadopoulos, *Combust. Flame*, **76**, 403 (1989).
10. G. G. De Soete, *Proc. Combust. Inst*., **15**, 1093 (1975).
11. J. Zhang, R. Sun and S. H. Wu, *Proceeding of the CSEE*, **23**, 215 (2003) (in Chinese).
12. T. H. Shih, W. W. Liou, A. Shabbir, Z. Yang and J. Zhu, *Computational Fluids*, **24**, 227 (1995).
13. Y. K. Qin,Q. Y. Zhu and T. Zhu, *Electric Power*, **33**, 14 (2000) (in Chinese).
14. T. S. Liu, W. Zhou and E. Q. Ye, *Power Engineering*, **26**, 116 (2006) (in Chinese).
15. L. S. Xiao, H. C. Zeng, F. Jin and J. Han, *Power Engineering*, **21**, 1043 (2001) (in Chinese).
16. H. Spliethoff, U. Greul, H. Rudiger and K. R. G. Klaus, *Fuel*, **75**, 560 (1996).